Novel Cyclometalated Iridium(III) Xanthate Complexes and Their Phosphorescence Behavior in the Presence of Metal Ions

Bihai Tong[a], Yaqing Xu[a], Jiayan Qiang[a], Man Zhang[a], Qunbo Mei[b], Hengshan Wang[c], and Qian-Feng Zhang[a]

[a] College of Metallurgy and Resources, Institute of Molecular Engineering and Applied Chemistry, Anhui University of Technology, Ma'anshan, Anhui 243002, P. R. China

[b] Jiangsu Key Lab of Organic Electronics & Information Displays, Institute of Advanced Materials (IAM), Nanjing University of Posts & Telecommunications (NUPT), Nanjing 210046, P. R. China

[c] Key Laboratory for the Chemistry and Molecular Engineering of Medicinal Resources, College of Chemistry & Chemical Engineering, Guangxi Normal University, Guilin 541004, P. R. China

Reprint requests to Dr. Qunbo Mei. Fax: +86-25-85866396. E-mail: iamqbmei@njupt.edu.cn

Z. Naturforsch. **2012**, *67b*, 865 – 871 / DOI: 10.5560/ZNB.2012-0119
Received May 5, 2012

Two cyclometalated iridium(III) complexes, Ir(dpppz)(ppz)(ipx) and Ir(ppz)$_2$(ipx) (dpppzH = 1-(2,6-dimethylphenoxy)-4-phenylphthalazine, ppzH = 4-phenylphthalazinone, ipx = isopropyl xanthate), have been synthesized and characterized by single-crystal X-ray diffraction. The photophysical properties of the two complexes were also investigated. Ir(dpppz)(ppz)(ipx) shows orange-red emission at around 606 nm with a phosphorescence quantum yield of *ca*. 0.0032 and an emission lifetime of 188 ns, while Ir(ppz)$_2$(ipx) shows orange-red emission at around 599 nm with a phosphorescence quantum yield of *ca*. 0.00318 and an emission lifetime of 259 ns. The phosphorescence behavior of Ir(ppz)$_2$(ipx) towards different metal cations has also be studied. Its strong phosphorescence is quenched by Hg^{2+}, Cu^{2+} and Ag^{+} cations. The interaction ratio with Hg^{2+} is 1:1.

Key words: Cyclometalated Iridium(III) Complex, Xanthate, Crystal Structure, Phosphorescence

Introduction

Recently, there is an increasing interest in the synthesis of cyclometalated Ir(III) complexes, which have found applications as phosphors in organic light emitting diodes (OLEDs) [1], sensors [2], and luminescent labels for biomolecules [3]. At the same time, sulfur-containing ligands, such as dithiophosphates, dithiocarbamates and dithiocarbonates, have great binding potential to metals and have a wide range of uses in coordination chemistry [4]. These ligands are capable of stabilizing metal ions in unusual oxidation states. For example, [Ir(R_2NCS_2)$_3$] can be oxidized reversibly to [Ir(R_2NCS_2)$_3$]$^+$ [5]. Dithiocarbonates are well known as heavy metal chelating agents and most common collector agents in the flotation process for sulfide minerals [6]. Cyclometalated Ir(III) complexes with dithiophosphate and dithiocarbamate ligands have been previously synthesized and used as phosphors in OLEDs [7 – 10]. However, cyclometalated Ir(III) dithiocarbonates have not been well explored.

We have been interested in novel cyclometalated iridium(III) complexes contaning xanthate ligands and to investigate their potential for heavy transition metal ion detection.

In the work presented here, two cyclometalated iridium(III) complexes, Ir(dpppz)(ppz)(ipx) and Ir(ppz)$_2$(ipx) (dpppzH = 1-(2,6-dimethylphenoxy)-4-phenylphthalazine, ppzH = 4-phenylphthalazinone, ipx = isopropyl xanthate) have been synthesized and characterized. The phosphorescence behavior of Ir(ppz)$_2$(ipx) towards different metal cations was also studied.

Experimental Section

General

All solvents were purified by routine procedures and distilled under an atmosphere of dry nitrogen before use. All reagents, unless otherwise specified, were purchased from Aldrich and were used as received. UV/Vis absorption spectra were recorded on a Shimadzu UV-2501 PC spectrophotometer. ESI mass spectra were recorded on a Perkin Elmer Sciex API 365 spectrometer. NMR spectra were recorded on a Bruker AV400 spectrometer. Photoluminescence (PL) spectra were measured with a Shimadzu RF-5301PC fluorescence spectrophotometer. Luminescence lifetimes were determined on an Edinburgh FL920 time-correlated pulsed single-photon-counting instrument.

Synthesis of the Iridium(III) complexes Ir(dpppz)(ppz)(ipx) and Ir(ppz)$_2$(ipx)

To a 25 mL round-bottomed flask, 2-ethoxyethanol (9 mL), 1-(2,6-dimethylphenoxy)-4-phenylphthalazine (dpppzH) (0.46 g, 1.40 mmol), $IrCl_3{\cdot}3H_2O$ (0.20 g, 0.56 mmol), and water (3 mL) were added sequentially. The mixture was stirred overnight under nitrogen at 110 °C and cooled to room temperature. The precipitate was collected and washed with ethanol and acetone, and then dried *in vacuo* to give red cyclometallated Ir(III)-μ-chloro-bridged dimers (0.27 g) [11]. The Ir(III)-μ-chloro dimers (0.27 g) and potassium isopropyl xanthate (0.17 g, 1.00 mmol) were dissolved in the mixed solvent of CH_2Cl_2-CH_3OH (15 : 15 mL). The resulting red solution was stirred for 4 h at room temperature. After the solution was washed three times with distilled water, the organic solution was evaporated to dryness and the residue purified by column chromatography using CH_2Cl_2-ethyl acetate (10 : 1, v:v). Ir(dpppz)(ppz)(ipx) was isolated with a yield (calculated with $IrCl_3{\cdot}3H_2O$ as starting material) of 8 % (0.037 g) and Ir(ppz)$_2$(ipx) with a yield of 39 % (0.170 g).

Ir(dpppz)(ppz)(ipx): ^{1}H NMR ($CDCl_3$, 400 MHz): δ = 1.35 (d, J = 6.0 Hz, 3H, CMe_2), 1.42 (d, J = 6.4 Hz, 3H, CMe_2), 2.24 (s, 6H, *OPh*-Me_2), 5.14 – 5.21 (m, 1H, $CHMe_2$), 6.47 (d, J = 7.6 Hz, 2H, $OPhMe_2$), 6.72 (t, J = 7.6 Hz, 1H, $OPhMe_2$), 6.83 (d, J = 3.6 Hz, 1H, Ph-H), 6.93 (t, J = 7.6 Hz, 1H, Ph-H), 6.98 – 7.02 (m, 1H, Ph-H), 7.07 (s, 3H, Ph-H), 7.87 (t, J = 8.0 Hz, 1H, Pz-H), 7.97 (t, J = 8.0 Hz, 1H, Pz-H), 8.03 – 8.21 (m, 3H, Ph-H and Pz-H), 8.21 (d, J = 8.0 Hz, 1H, Ph-H), 8.66 (d, J = 7.6 Hz, 1H, Pz-H), 8.70 (d, J = 7.2 Hz, 1H, Pz-H), 8.76 (d, J = 8.3 Hz, 1H, Pz-H), 9.00 (d, J = 9.5 Hz, 1H, Pz-H). – ^{13}C NMR ($CDCl_3$, 100 MHz): δ = 163.49 (OCS_2), 159.13, 157.89 ($OC{=}N$), 155.77, 155.32 (C=*N*), 154.63, 150.31, 142.13, 141.96, 133.56, 132.93, 132.35, 132.23, 131.63 (Pz), 129.62, 129.36, 129.17, 128.80, 128.30, 128.28, 127.86, 126.15, 125.70 (Ph), 125.51, 123.90, 121.48, 121.14, 120.67, 119.48 ($OPhMe_2$), 21.92 (CH_3), 21.50 (CH_3), 16.61 ($CHMe_2$). – MS ((+)-ESI): m/z = 815 (calcd. 815 for $C_{37}H_{26}N_4O_2S_2Ir$, $[M–i\mathrm{PrO}]^+$).

Ir(ppz)$_2$(ipx): ^{1}H NMR ($CDCl_3$, 400 MHz): δ = 1.52 (d, J = 6.4 Hz, 3H, CMe_2), 1.58 (d, J = 6.0 Hz, 3H, CMe_2), 5.60 – 5.66 (m, 1H, $CHMe_2$), 6.82 – 6.88 (m, 4H, Ph-H), 7.02 (t, J = 8.0 Hz, 2H, Ph-H), 7.93 (t, J = 7.6 Hz, 2H, Pz-H), 8.02 (t, J = 8.0 Hz, 2H, Pz-H), 8.12 (d, J = 8.0 Hz, 2H, Ph-H), 8.68 (d, J = 8.0 Hz, 2H, Pz-H), 8.79 (d, J = 8.0 Hz, 2H, Pz-H). – ^{13}C NMR ($CDCl_3$, 100 MHz): δ = 158.98 (OCS_2), 156.67 ($OC{=}N$), 151.60 (C=*N*), 141.66, 133.89, 132.30, 132.04, 129.37, 129.28 (Phz), 128.41, 128.38, 127.98, 126.47, 122.07 (Ph), 21.68 (CH_3), 21.60 (CH_3), 14.21 ($CHMe_2$). – MS ((-)-ESI): m/z = 769 (calcd. 769 for $C_{32}H_{24}N_4O_3S_2Ir$, $[M–H]^-$).

Titration procedure

Spectrophotometric titrations were performed in a CH_3CN-H_2O (10 : 1, v:v) solution of Ir(ppz)$_2$(ipx) (2 mL of a 10^{-5} M solution). Typically, aqueous solutions (0.01 M) of freshly prepared perchlorate salts of metal cations (Hg^{2+}, Fe^{2+}, Cu^{2+}, Co^{2+}, Ni^{2+}, Zn^{2+}, Pb^{2+}, Cr^{3+}, Ag^+, Cd^{2+} and Mg^{2+}) were added, and the UV/Vis absorption and fluorescence spectra of the samples were recorded on a Shimadzu UV/Vis spectrophotometer and a Hitachi F-4600 fluorescence spectrophotometer at room temperature after 1 min.

Crystal structure determination

Single crystals of Ir(dpppz)(ppz)(ipx) and Ir(ppz)$_2$(ipx) were obtained by repeated recrystallization using a mixture of CH_2Cl_2 and hexane at room temperature, and then mounted on glass fibers. Diffraction data were collected on a Bruker SMART Apex CCD diffractometer with Mo K_α radiation (λ = 0.71073 Å) at 296 K using an ω scan mode. Crystallographic and experimental data of Ir(dpppz)(ppz)(ipx) and Ir(ppz)$_2$(ipx) are listed in Table 1.

CCDC 821427 and 821670 contain the supplementary crystallographic data for this paper. These data can be obtained free of charge from The Cambridge Crystallographic Data Centre *via* www.ccdc.cam.ac.uk/data_request/cif.

Results and Discussion

The neutral cyclometalated iridium(III) complexes Ir(dpppz)(ppz)(ipx) and Ir(ppz)$_2$(ipx) were readily prepared from the Ir(III)-μ-chloro-bridged dimers [11] and potassium isopropyl xanthate at room temperature (Fig. 1). Both complexes were characterized by MS and NMR spectroscopy. In the ^{1}H NMR spectrum of Ir(dpppz)(ppz)(ipx), the six protons of the

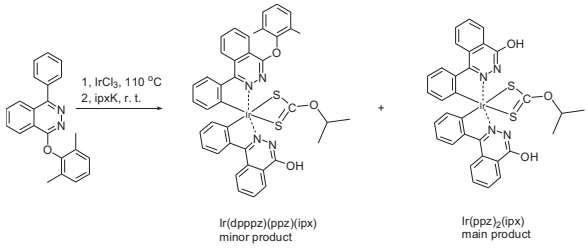

Fig. 1. Synthesis of the iridium(III) complexes.

methyl groups on phenoxy appeared at 2.24 ppm, and the three phenoxy protons appeared at 6.47 and 6.72 ppm, while these peaks disappeared totally in $Ir(ppz)_2(ipx)$, which indicated a partly hydrolysis of the phenoxy group in Ir(dpppz)(ppz)(ipx) and an entirely hydrolyzation in $Ir(ppz)_2(ipx)$. Because Ir(dpppz)(ppz)(ipx) was the minor and $Ir(ppz)_2(ipx)$ was the main product, it could be deduced that most of the cyclometalated ligands hydrolyzed during the reflux reaction of the ligands and $IrCl_3 \cdot 3H_2O$ [11]. Actually, if the 2,6-dimethylphenoxy group was replaced by a phenoxy group, no cyclometalated iridium(III) complex could be obtained, and the cyclometalated ligands underwent complete hydrolysis. The total integral of the 4-phenylphthalazine ligands in the low-field range was consistent with a theoretical value of 16 H. The diastereotopic nature of the xanthate methyl groups has also been found in the NMR signal non-equivalence. The ^{1}H and ^{13}C NMR chemical shift differences of the methyl groups were found separately as 0.07 and 0.42 ppm for Ir(dpppz)(ppz)(ipx), 0.06 and 0.08 ppm for $Ir(ppz)_2(ipx)$, indicating that there are equal amounts of both enantiomers of two complexes.

The structures of Ir(dpppz)(ppz)(ipx) and $Ir(ppz)_2(ipx)$ have been further confirmed by X-ray crystallography. As shown in Figs. 2 and 3, both complexes have distorted octahedral coordination geometry around iridium by two cyclometalated ligands and one ipx ligand with *cis*-C–C and *trans*-N–N dispositions. The Ir–C bond lengths, ranging from

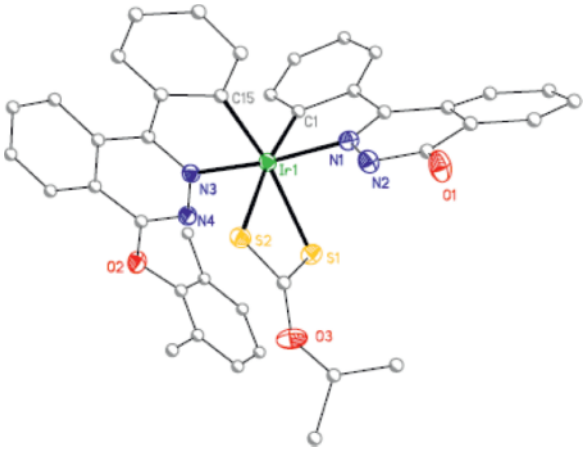

Fig. 2 (color online). Perspective view of Ir(dpppz)(ppz)(ipx). Displacement ellipsoids are shown at the 25% probability level. Selected distances (Å) and angles (deg): C(1)–Ir(1) 2.011(5), C(15)–Ir(1) 1.994(6), Ir(1)–N(3) 2.020(4), Ir(1)–N(1) 2.028(5), Ir(1)–S(2) 2.4731(16), Ir(1)–S(1) 2.4757(17); C(15)–Ir(1)–C(1) 91.4(2), C(15)–Ir(1)–N(3) 79.2(2), C(1)–Ir(1)–N(3) 95.5(2), C(15)–Ir(1)–N(1) 97.33(19), C(1)–Ir(1)–N(1) 78.5(2), N(3)–Ir(1)–(1) 173.1(2), C(15)–Ir(1)–S(2) 95.27(18), C(1)–Ir(1)–S(2) 171.99(14), N(3)–Ir(1)–S(2) 90.19(16), N(1)–Ir(1)–S(2) 96.12(15), C(15)–Ir(1)–S(1) 166.60(17), C(1)–Ir(1)–S(1) 101.99(15), N(3)–Ir(1)–S(1) 98.18(14), N(1)–Ir(1)–S(1) 86.52(15), S(2)–Ir(1)–S(1) 71.51(5).

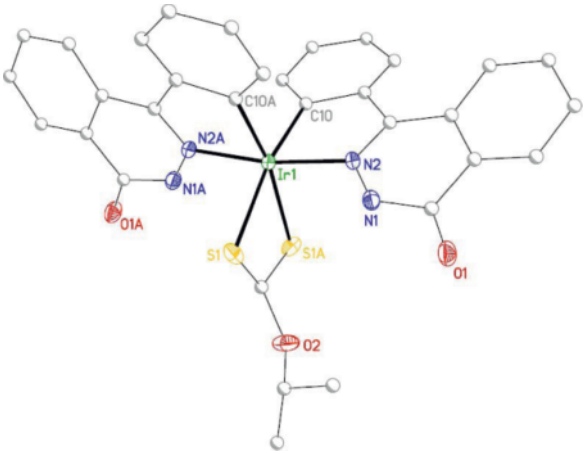

Fig. 3 (color online). Perspective view of $Ir(ppz)_2(ipx)$. The complex has crystallographic C_2 (2) symmetry with the O*i*Pr group being two-fold disordered. Displacement ellipsoids are shown at the 25% probability level. Selected distances (Å) and angles (deg): C(10)–Ir(1) 2.023(6), Ir(1)–N(2) 2.024(5), Ir(1)–N(2)A 2.024(5), Ir(1)–C(10)A 2.023(6), Ir(1)–S(1)A 2.4819(15), Ir(1)–S(1) 2.4819(15); N(2)–Ir(1)–N(2) A 170.5(2), N(2)–Ir(1)–C(10)A 94.7(2), N(2)A–Ir(1)–C(10)A 78.8(2), N(2)–Ir(1)–C(10) 78.8(2), N(2)A–Ir(1)–C(10) 94.7(2), C(10)A–Ir(1)–C(10) 93.3(4), N(2)–Ir(1)–S(1)A 90.91(14), N(2)A–Ir(1)–S(1)A 96.79(14), C(10)A–Ir(1)–S(1)A 168.21(18), C(10)–Ir(1)–S(1)A 97.93(18), N(2)–Ir(1)–S(1) 96.79(14), N(2)A–Ir(1)–S(1) 90.91(14), C(10)A–Ir(1)–S(1) 97.93(18), C(10)–Ir(1)–S(1) 168.21(18), S(1)A–Ir(1)–S(1) 71.07(8). Symmetry code: A $-x, y, 1/2 - z$.

Table 1. Crystal data, data collection and structure refinement parameters for Ir(dpppz)(ppz)(ipx) and $Ir(ppz)_2(ipx)$.

Compound	Ir(dpppz)(ppz)(ipx)	$Ir(ppz)_2(ipx)$
Formula	$C_{40}H_{33}IrN_4O_3S_2$	$C_{32}H_{25}IrN_4O_3S_2$
M_r	874.02	769.88
Crystal size, mm^3	$0.43 \times 0.20 \times 0.03$	$0.23 \times 0.23 \times 0.11$
Crystal system	monoclinic	monoclinic
Space group	*Cc*	*C*2/*c*
a, Å	8.8718(4)	20.5757(7)
b, Å	23.0562(10)	11.2281(4)
c, Å	17.7776(9)	17.0882(9)
β, deg	103.225(3)	126.128(2)
V, $Å^3$	3540.0(3)	3188.7(2)
Z	4	4
D_{calcd}, g cm^{-3}	1.64	1.60
μ (MoK_α), cm^{-1}	43.6	39.4
F(000), e	1736	1512
θ range for data collection, deg	1.77 – 27.00	2.19 – 27.42
hkl range	±11, −25 → 29, −22 → 14	±26, −13 → 14, ±22
Refl. measured/unique/R_{int}	16 261/5422/0.0352	14 930/3636/0.0276
Param. refined	402	197
$R(F)/wR(F^2)$ (all refl.)	0.0338/0.0642	0.0460/0.1254
GoF (F^2)	1.018	1.164
Largest diff. peak/hole, e $Å^{-3}$	1.12/−0.53	2.62/−1.06

1.994 to 2.023 Å, are shorter than the Ir–N bonds spanning from 2.020 to 2.024 Å. This result implies that there is a stronger *trans* influence of the phenyl over that of the phthalazine group [12]. The Ir–S bond lengths are ranging from 2.4731 to 2.4819 Å. Ir(dpppz)(ppz)(ipx) (non-centrosymmetric space group) forms homochiral crystals, and in the batch there are equal amounts of crystals each consisting entirely of one enantiomer (*R* in the crystal examined). $Ir(ppz)_2(ipx)$ (centrosmmetric space group) has equal amounts of both *R* and *S* enantiomers in one single crystal. Furthermore, the C–C and C–N bond lengths and angles are within normal ranges and are in agreement with the corresponding parameters as described for similarly constituted complexes [13 – 15].

The UV/Vis absorption spectrum of Ir(dpppz)(ppz)(ipx) in CH_2Cl_2 (Fig. 4) is dominated by an intense absorption at *ca.* 250 – 350 nm and a comparatively less intense band at *ca.* 350 – 437 nm which tails off to *ca.* 440 – 570 nm. The former is assigned to typical spin-allowed $^1\pi$-π^* transitions of the ligands, and the latter to LLCT and ^{1}MLCT transition. The band at 450 nm may be assigned to the formally spin-forbidden ^{3}MLCT transition. Compared to Ir(dpppz)(ppz)(ipx), the corresponding absorption bands of complex $Ir(ppz)_2(ipx)$ have an obvious blue-shift after the partial hydrolysis of the cyclometalated ligand, which is consistent with the reduction of the conjugated π system in the ligands.

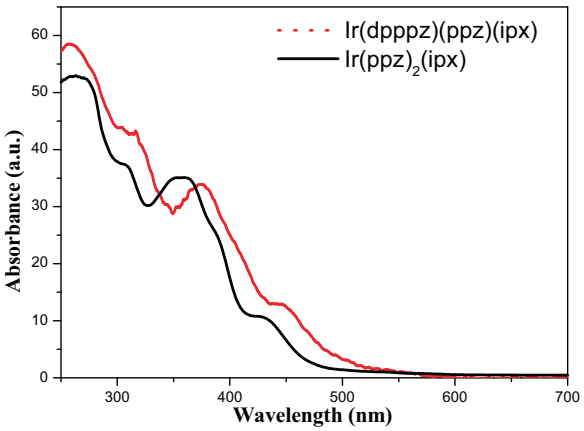

Fig. 4 (color online). UV/Vis absorption spectra of the iridium(III) complexes in CH_2Cl_2.

The room-temperature photoluminescence spectra of the complexes Ir(dpppz)(ppz)(ipx) and $Ir(ppz)_2(ipx)$ in CH_2Cl_2 solution are illustrated in Fig. 5. Ir(dpppz)(ppz)(ipx) emits an intense luminescence with the emission wavelength at 606 nm, while that of $Ir(ppz)_2(ipx)$ is blue-shifted to 599 nm, which is consistent with the UV/Vis absorption result. The excited state lifetime of Ir(dpppz)(ppz)(ipx) in CH_2Cl_2 solution has been determined to be 188 ns and

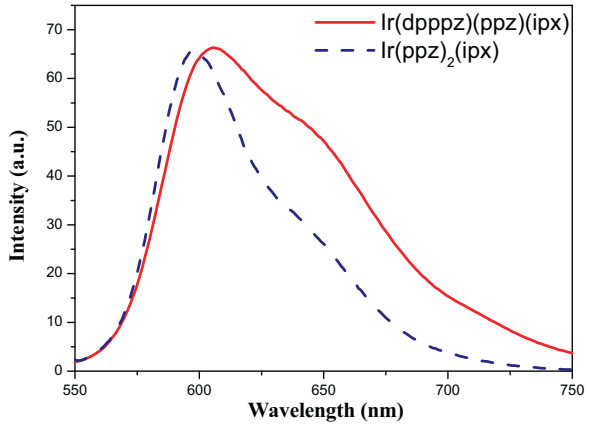

Fig. 5 (color online). The room-temperature photoluminescence spectra of the complexes in CH_2Cl_2 solution ($\lambda_{ex} = 420$ nm).

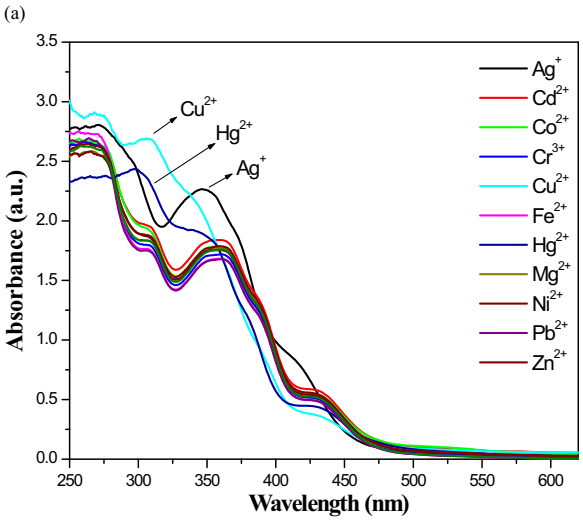

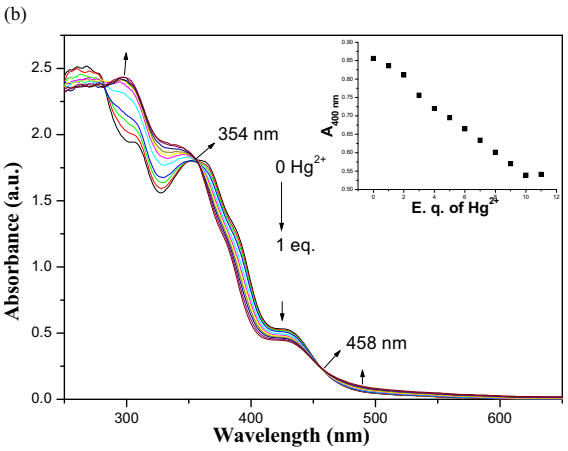

Fig. 6 (color online). The UV/Vis absorption spectra of $Ir(ppz)_2(ipx)$ in the presence of 2 equiv. of different metal ions (a) and changes upon addition of Hg^{2+} (b).

that of $Ir(ppz)_2(ipx)$ 259 ns. Both are obviously shorter than that of $[Ir(ppy)_3]$ (ppy = phenylpyridinato) (2.0 μs) [16]. The phosphorescence quantum efficiency of Ir(dpppz)(ppz)(ipx) in CH_2Cl_2 is *ca.* 0.0032, and that of $Ir(ppz)_2(ipx)$ is 0.00318, using an aqueous solution of $[Ru(bpy)_3]Cl_2$ ($\Phi = 0.042$) as the standard [17]. The presence of S atoms in these complexes is responsible for the weak luminescence intensity due to their heavy atom effects [18].

In order to explore the metal cation sensor potential of $Ir(ppz)_2(ipx)$, the UV/Vis absorption and phosphorescence behavior towards different transition metal cations have been investigated.

Fig. 6(a) shows the effects of different metal cations (Hg^{2+}, Ag^{+}, Cu^{2+}, Fe^{2+}, Co^{2+}, Ni^{2+}, Zn^{2+}, Mg^{2+}, Cr^{3+}, Pb^{2+} and Cd^{2+}) on the UV/Vis absorption spectral properties of $Ir(ppz)_2(ipx)$. Hg^{2+} has a pronounced effect on the spectra of $Ir(ppz)_2(ipx)$, with the less intense band at *ca.* 350 – 437 nm having an obvious blue shift. Similar changes were also observed when Cu^{2+} and Ag^{+} were added, indicating strong complexation interactions between $Ir(ppz)_2(ipx)$ and the Hg^{2+}, Ag^{+} and Cu^{2+} cations. The other metal ions had nearly no influence on the UV/Vis absorption spectra of $Ir(ppz)_2(ipx)$**.** In order to explore the quantitative interrelation of $Ir(ppz)_2(ipx)$ with Hg^{2+}, the changes in the UV/Vis absorption spectra (Fig. 6(b)) were investigated by titration experiments. Upon addition of Hg^{2+}, the absorption bands of $Ir(ppz)_2(ipx)$ at 354 – 458 nm gradually decreased, and a new band centered at 300 nm started to develop with two distinct isosbestic points at 354 and 458 nm, indicating strong ground state interactions between $Ir(ppz)_2(ipx)$ and Hg^{2+}. The stoichiometry of $Ir(ppz)_2(ipx)$ is given by the variation of $A_{400\ nm}$ with respect to the equivalents of Hg^{2+} added (Fig. 6(b) inset). Effectively, $A_{400\ nm}$ decreases continuously up to 1 equiv. of Hg^{2+}. Further addition of Hg^{2+} induces only very minor changes in $A_{400\ nm}$, indicating that $Ir(ppz)_2(ipx)$ has a 1 : 1 interaction with Hg^{2+}.

Fig. 7(a) shows the effects of different metal cations on the fluorescence properties of $Ir(ppz)_2(ipx)$. When

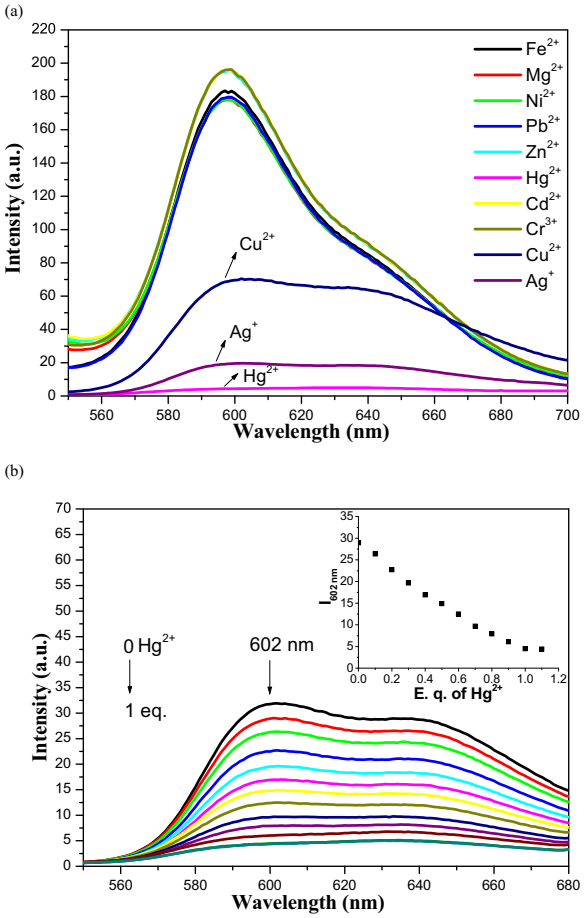

Fig. 7 (color online). The emission spectra of $Ir(ppz)_2(ipx)$ in the presence of 2 equiv. of different metal ions (a) and changes upon addition of Hg^{2+} (b).

2 equiv. of Hg^{2+} were added, the luminescence intensity at 599 nm decreased to 3 %. Similar changes were also observed when Ag^{+} and Cu^{2+} were added, and the luminescence intensity decreased to 10 % and 35 %, respectively, indicating strong interactions. However, no obvious spectral variations were measured upon addition of other metal cations. The emission spectral change for the interaction of $Ir(ppz)_2(ipx)$ with Hg^{2+} has also been studied. It can be seen from Fig. 7(b) that the emission decreases continuously up to *ca.* 1 equiv. of Hg^{2+}. Addition of excess Hg^{2+} to $Ir(ppz)_2(ipx)$ leads to only minor changes, suggesting a 1:1 ratio for the binding of $Ir(ppz)_2(ipx)$ to Hg^{2+}, which is consistent with the UV/Vis absorption result. This phenomenon could be explained by the fact that Hg^{2+} (soft acid) interacts preferentially with sulfur (soft base) according to Pearson's hard and soft acids and bases theory [19]. It is well known that many heavy transition metal ions are typical fluorescence quenchers due to their paramagnetic nature and the heavy atom effect [20]. In fact, during the addition precipitates were generated. A mechanistic study on this phenomenon is currently in progress.

In summary, we have synthesized two cyclometalated iridium(III) complexes with xanthate as ancillary ligand. The complex $Ir(ppz)_2(ipx)$ shows a strong interaction with Hg^{2+}, Ag^{+} and Cu^{2+} cations, and the interaction ratio with Hg^{2+} is 1:1. Thus, the present results have shown that a design of highly selective chemosensors for metal cations by adjusting the cyclometalated ligands and xanthate ancillary groups is promising.

Acknowledgement

This project was supported by the National Natural Science Foundations of China (no. 50903001), the 973 project (no. 2011CB512005) and the Guangxi Natural Science Foundation of China (no. 2011GXNSFD018010).

[1] L. X. Xiao, Z. J. Chen, B. Qu, *Adv. Mater.* **2011**, *23*, 926 – 952.
[2] Q. Zhao, F. Y. Li, C. H. Huang, *Chem. Soc. Rev.* **2010**, *39*, 3007 – 3030.
[3] Q. Zhao, C. H. Huang, F. Y. Li, *Chem. Soc. Rev.* **2011**, *40*, 2508 – 2524.
[4] A. A. Mohamed, I. Kani, A. O. Ramirez, *Inorg. Chem.* **2004**, *43*, 3833 – 3839.
[5] A. M. Bond, R. Colton, B. M. Gatehouse, *Inorg. Chim. Acta* **1997**, *260*, 61 – 71.
[6] I. I. Ozturk, S. K. Hadjikakou, N. Hadjiliadis, *Inorg. Chem.* **2009**, *48*, 2233 – 2245.
[7] L. Q. Chen, H. You, C. L. Yang, *J. Mater. Chem.* **2006**, *16*, 3332 – 3339.
[8] L. Q. Chen, C. L. Yang, M. Li, J. G. Qin, *Cryst. Growth Des.* **2007**, *7*, 39 – 46.
[9] L. Q. Chen, C. L. Yang, J. G. Qin, J. Gao, *Synthetic Met.* **2005**, *152*, 225 – 228.
[10] M. K. Lau, K. M. Cheung, Q. F. Zhang, *J. Organomet. Chem.* **2004**, *689*, 2401 – 2410.

[11] B. H. Tong, J. Y. Qiang, Q. B. Mei, *Inorg. Chem. Commun.* **2012**, *17*, 113 – 115.
[12] B. Douglas, D. McDaniel, J. Alexander, *Concepts and Models in Inorganic Chemistry*, 3rd ed., John Wiley & Sons, New York, **1994**.
[13] M. Graf, M. Thesen, H. Krüger, P. Mayer, *Inorg. Chem. Commun.* **2009**, *12*, 701 – 703.
[14] B. H. Tong, F. H. Wu, Q. B. Mei, *Z. Naturforsch.* **2010**, *65b*, 511 – 515.
[15] B. H. Tong, Q. B. Mei, S. J. Wang, *J. Mater. Chem.* **2008**, *18*, 1636 – 1639.
[16] A. Tsuboyama, H. Iwawaki, M. Furugori, T. Mukaide, *J. Am. Chem. Soc.* **2003**, *125*, 12971 – 12979.
[17] J. van Houten, R. J. Watts, *J. Am. Chem. Soc.* **1976**, *98*, 4853 – 4858.
[18] T. Y. Ohulchanshyy, D. J. Donnelly, M. R. Detty, *J. Phys. Chem. B.* **2004**, *108*, 8668 – 8672.
[19] A. W. Varnes, R. B. Dodson, E. L. Wehry, *J. Am. Chem. Soc.* **1972**, *94*, 946 – 950.
[20] K. W. Huang, H. Yang, Z. G. Zhou, *Org. Lett.* **2008**, *10*, 2557 – 2560.